JACS
JOURNAL OF THE AMERICAN CHEMICAL SOCIETY

ARTICLE

pubs.acs.org/JACS

Pulsed Pressure Perturbations, an Extra Dimension in NMR Spectroscopy of Proteins

Werner Kremer,[†] Martin Arnold,[†,‡] Claudia Elisabeth Munte,[§] Rainer Hartl, Markus Beck Erlach, Joerg Koehler, Alexander Meier, and Hans Robert Kalbitzer*

Institute of Biophysics and Physical Biochemistry and Centre of Magnetic Resonance in Chemistry and Biomedicine (CMRCB), University of Regensburg, Universitätsstrasse 31, D-93047 Regensburg, Germany

Supporting Information

ABSTRACT: The introduction of multidimensional NMR spectroscopy was a breakthrough in biological NMR methodology because it allowed the unequivocal correlation of different spin states of the system. The introduction of large pressure perturbations in the corresponding radio frequency (RF) pulse sequences adds an extra structural dimension into these experiments. We have developed a microprocessor-controlled pressure jump unit that is able to introduce fast, strong pressure changes at any point in the pulse sequences. Repetitive pressure changes of 80 MPa in the sample tube are thus feasible in less than 30 ms. Two general forms of these experiments are proposed here, the pressure perturbation transient state spectroscopy (PPTSS) and the pressure perturbation state correlation spectroscopy (PPSCS). PPTSS can be used to measure the rate constants and the activation energies and activation volumes for the transition between different conformational states including the folded and unfolded state of proteins, for polymerization−depolymerization processes, and for ligand binding at atomic resolution. PPSCS spectroscopy correlates the NMR parameters of different pressure-induced states of the system, thus allowing the measurement of properties of a given pressure induced state such as a folding intermediate in a different state, for example, the folded state. Selected examples for PPTSS and PPSCS spectroscopy are presented in this Article.

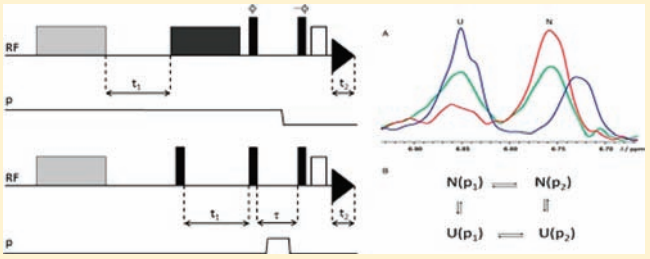

INTRODUCTION

The success of NMR spectroscopy in biological science is closely coupled to the invention of multidimensional spectroscopy. The combination of different RF and gradient pulses in appropriate acquisition schemes allows for the correlation of properties of nuclear spins of the system such as *J*-couplings and dipolar couplings and for one to deduce structural information of the macromolecule under consideration of their analysis. An interesting concept that expands the possibilities of the pure RF- and magnetic gradient-based multidimensional NMR spectroscopy is the introduction of additional pulsed perturbations in the sequence creating new physical dimensions. In principle, any physical perturbation such as light, heat, and pressure can be used that initiates chemical reactions or primarily influences the structural states and thus indirectly the spin system under consideration. However, for protein structural studies, the application of high hydrostatic pressures inside an NMR spectrometer has distinct advantages: it leads to a reversible perturbation of the corresponding thermodynamic equilibria and can be used for the study of excited conformational states of proteins, protein folding, protein aggregation, and ligand interaction at atomic resolution.[1] Rare "excited" conformational states can be stabilized by pressure; an example is the detection of an intermediate on the pathway of fibril formation of human prion protein that has a relative population of 0.0005 at ambient pressure.[2]

A time-dependent pressure perturbation can be introduced in NMR spectroscopy by manually changing the static pressure of the system. Here, only slow processes in the time range of minutes to days can be observed, and the pressure jump cannot be inserted in a pulse sequence.[3] The only method to obtain a better time resolution is the use of a spectrometer-controlled fast pressure−jump system. Most recently, Heuert et al.[4] have presented a home-built probe-head that is able to perform under computer-control a pressure step from high pressure to ambient pressure in the millisecond-time scale. They followed the spectral changes after a step from 10 MPa to ambient pressure by 1D NMR spectroscopy. For protein NMR, much higher pressure steps and the design of more involved NMR experiments are required.[5]

EXPERIMENTAL SECTION

NMR Samples. Uniformly ^{15}N enriched histidine-containing phosphocarrier protein (HPr) from *S. aureus* was produced according to

Received: June 1, 2011
Published: July 21, 2011

dx.doi.org/10.1021/ja2050698 | *J. Am. Chem. Soc.* 2011, 133, 13646–13651

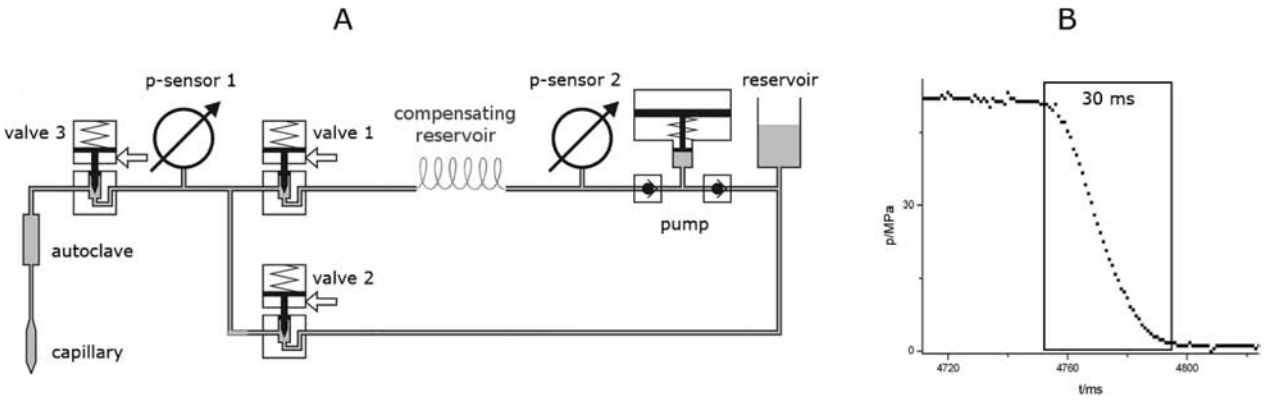

Figure 1. Schematic view and performance of the pressure jump apparatus. (A) The microprocessor-controlled pressure jump system; (B) the pressure response measured at sensor 1.

Maurer et al.[6] The sample contained 3 mM HPr, 0.1 mM DSS in 90% H_2O/10% D_2O, pH 7.0. Data were measured at T = 295 K. HPr(I14A) from *S. carnosus* was obtained as described by Möglich et al.[7] The NMR sample contained approximately 1.5 mM HPr(I14A) in 10 mM Tris-d_{11} pH 7.0, 0.5 mM EDTA-d_6, 0.5 mM NaN_3, 99.8% D_2O. Data were measured at T = 285 K. The three-dimensional structures of the two proteins were solved by NMR[6,7] and are deposited in the Protein Data Base, accession numbers 1KA5 and 1TXE.

NMR Spectroscopy. All NMR spectra were recorded with a Bruker Avance-500 NMR spectrometer operating at a proton ^1H NMR frequency of 500.1 MHz. Measurements were performed in a 5 mm triple resonance probe (TXI) using a homemade borosilicate sample cell (PPTSS-experiments) or a ceramic cell (Daedalus Innovations, Philadelphia, PA) (PPSCS-experiments). The borosilicate cell was connected to the system by a homemade titanium autoclave, and the pressure was transduced to the sample by a capped Teflon tube.[8] For the ceramic tube, the autoclave provided by the manufacturer was used that was slightly modified by separating the pressurized methylcyclohexane from the aqueous sample by a thin polyethylene membrane.

Pressure inside the NMR cell was measured by using the pressure-dependent chemical shift changes of histidine $H^{\varepsilon 1}$ protons, and pressure jump induced temperature changes were measured by the chemical shift difference of the hydroxyl and methylene protons of ethylene glycol calibrated for different pressures.[9]

^{15}N chemical shifts were indirectly referenced to DSS.[10] PPTSS-experiments were performed using a pressure jump followed after varying times t by a 1D NOESY pulse sequence including a WATERGATE W5 solvent suppression.[11,12] The repetition time used was 15 s, the spectral width was 12.0161 ppm, and 16 384 time domain data points were recorded. 128 scans were used per time point leading to a total experimental time of 32 min. The pulse sequence is given in Figure 2B.

The 2D ^1H,^{15}N HSQC (heteronuclear single quantum coherence) spectrum was recorded with a pulse sequence described by Bax et al.[13] modified by a set of two $\pi/2$ pulses separated by 100 ms with phases ϕ and $-\phi$. During this time, a pressure step was performed. The repetition time used was 7 s, the spectral widths were 16.0214 and 36 ppm, and the size of the time domain data was 4096 × 256 points in the ^1H and ^{15}N dimension, respectively. 40 FIDs were summed per time increment, leading to a total experimental time of 4 h 30 min. The water presaturation was set to 1 s, the interval Δ for the INEPT transfer was set to $1/4J$ (2.6 ms), the interval for the pressure jump was set to 100 ms, the optional additional water saturation pulse was switched off, the delay d4 was set to 0.5 ms, the gradients G had a duration of 1 ms, and the strengths G_1, G_2, and G_3 were 10%, 34%, and 22% of the maximum values. ^{15}N decoupling was performed with the Garp sequence.[14] This sequence is given in Figure 2D.

Data Evaluation. The relative concentrations c_U/c_T and c_N/c_T as a function of the time t after the pressure perturbation were fitted as a function of the waiting time t to the function:

$$c_N(t)/c_T = \tau_e k_{UN} - (\tau_e k_{UN} - c_N(t_0)/c_T)\exp\left(-\frac{t-t_0}{\tau_e}\right)$$

$$= \tau_e k_{UN} - a\exp\left(-\frac{t}{\tau_e}\right)$$

with the exchange correlation τ_e defined by $(1/(\tau_e)) = k_{NU} + k_{UN}$. c_N, c_U, and c_T are the concentrations of the natively folded protein (N), the unfolded protein (U), and the total concentration of the protein, t_0 is the time offset, and a comprises the pre-exponential factor that is not time dependent. k_{NU} and k_{UN} are the rate constants for transitions from N to U and U to N, respectively.

RESULTS AND DISCUSSION

We have developed a microprocessor-controlled pressure jump unit that is able to perform short rapid pressure steps with a slope of more than 25 GPa/s at the sample that can be fully integrated in the NMR pulse programs (Figure 1). A similar system was used earlier for small-angle X-ray scattering (SAXS) measurements.[15] Our system consists of a high pressure cell inserted into the NMR probe that is connected via high pressure tubes to the high pressure pump. A pressurized liquid (in our case methylcyclohexane) is transmitted via a separator (the Teflon tube and the polyethylene membrane, respectively) to the sample that in structural biology is usually an aqueous solution of a protein. Valve 3 is a safety valve that is closed automatically when the high pressure cell is exploding (a case that happens sometimes because the maximum pressure used for proteins is close to the limit of currently available materials) or can be closed by the operator in the case of emergency. When valve 1 is opened and valve 2 is closed, the pressure created by the pump is transmitted to the sample, while closing of valve 1 and opening of valve 2 resets the pressure to atmospheric pressure (for more details, see the Supporting Information).

Because the opening and closing of the valves is microprocessor controlled, it can be inserted at any point in the standard NMR pulse programs. The pressure response measured with sensor 1 (Figure 1B) is mainly limited by the switching time of the high pressure valves; for a pressure step of 80 MPa, about 30 ms is required. The separators used in our system were shown to have no influence on the pressure response measured in the

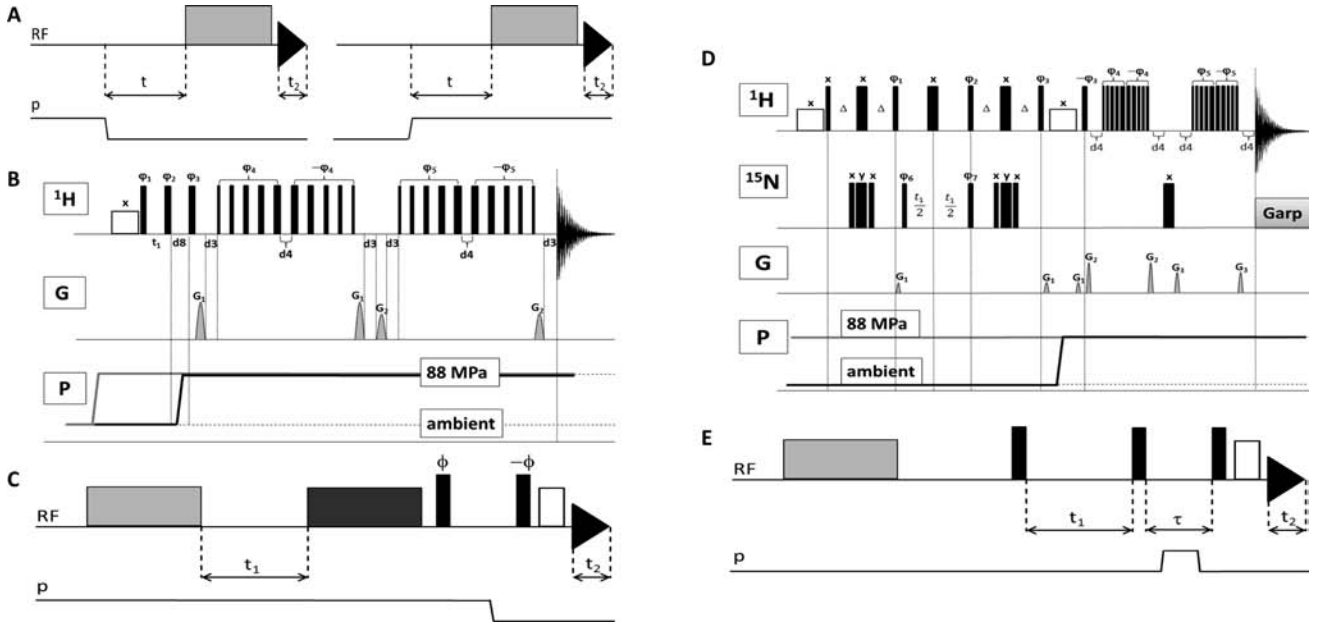

Figure 2. Dynamic pressure perturbation spectroscopy. General pulse sequences (A) for pressure perturbation transient state spectroscopy (PPTSS) and (C and E) for pressure perturbation correlation spectroscopy (PPSCS). The light and dark gray rectangles symbolize a series of RF and magnetic gradient pulses, the triangle the free induction decay (FID), the black rectangles $\pi/2$ − RF pulses with phases ϕ, and the black bordered white rectangle a water suppression pulse sequence. The times t and t_1 are varied from experiment to experiment; the interval τ is the time required for performing the pressure step or pulse. During this time, also a magnetic gradient pulse is applied for destroying transversal magnetization. During the time t_2, the signal is recorded. (B) Pulse sequences for a 1D ^{1}H PPTSS experiment and a 2D-^{1}H-NOESY-PPSCS-experiment. G, magnetic field gradients, P, pressure, (thin line) for PPTSS, (thick line) for PPSCS. Phase cycling $\phi_1 = (x, -x)$, $\phi_2 = (x)$, $\phi_3 = (x)$, $\phi_4 = (x, x, y, y, -x, -x, -y, -y)$, $\phi_5 = (8(x), 8(y), 8(-x), 8(-y)$, receiver phase $(2(x, -x, -x, x), 2(-x, x, x, -x)$, phase ϕ_1 is incremented for phase-sensitive detection with TPPI by 90° for every time increment. For the 1D experiment, t_1 is set to a constant value (3 μs), while for a 2D experiment, t_1 is incremented. The low power pulse (x) for water saturation is omitted for PPTSS. The delay d8 is 10 ms for PPTSS, larger than the time needed for the pressure jump (typically 50 ms) for PPSCS. Gradient durations 1 ms, gradient strengths $G_1 = 34\%$, $G_2 = 22\%$ of the maximum strength. The delay d3 was set to 0.5 ms in Figure 3 but could be reduced to 0.1 ms. Delay d4 determines the excitation spectrum and was set to 0.25 ms in the experiment shown in Figure 3. (D) PPSCS-HSQC pulse sequence, G, magnetic field gradient, Garp, ^{15}N broadband decoupling. Phases cycling $\phi_1 = (y, -y)$, $\phi_2 = (4(x), 4(-x))$, $\phi_3 = (-y, y, y, -y)$, $\phi_4 = (y, y, -y, -y, -x, -x, x, x)$, $\phi_5 = (8(y), 8(-x), 8(-y), 8(x))$, $\phi_6 = (x, x, -x, -x)$, $\phi_7 = (x, x, -x, -x)$, receiver phase $(x, -x, -x, x, x, x, x, -x, -x, x, x, -x, x, -x, -x, x)$, phase ϕ_6 is incremented for phase-sensitive detection with TPPI by 90° for every time increment. (E) PPSCS-NOESY.

sample.[9] Compression of liquids leads to an increase of temperature in the sample during the compression. The temperature increase during a pressure jump of 80 MPa is < 1 K as determined with an NMR sample (see the Experimental Section). Because the subsequent pressure decrease leads to an expansion and thus to a corresponding cooling of the sample, in first approximation during a repetitive experiment, no net warming occurs in a full pressure cycle. Several materials can be used for the production of high pressure cells; for static high pressure experiments initially quartz capillaries[16] were used, while other cells were made of sapphire single crystals[17,18] or ceramics.[19,20] Because the small inner diameters of the quartz capillaries add an additional friction to the system (and thus increase the switching time by 10−20 ms), ceramic cells are best suited for pressure jump experiments. Sapphire cells cannot be used because they are usually destroyed after several thousand pressure jumps by the high pressure gradients. In general, two different types of dynamic pressure perturbation experiments can be performed. In the first type, the pressure change is performed before starting the pulse sequence (pressure perturbation transient state spectroscopy, PPTSS); in the second type, the pressure change is performed during the NMR-pulse sequence (pressure perturbation state correlation spectroscopy, PPSCS) (Figure 2). The PPTSS experiment measures the time-dependent pressure response of a biological system after a periodic perturbation. In contrast to normal NMR experiments, a nonequilibrium system is established here. Possible applications of PPTSS are the determination of rate constants in folding/unfolding experiments, of free activation energies and activation volumes for conformational changes, ligand binding, and polymerization reactions. Another possibility we propose here is the use of more general perturbations such as the reversible destruction of the order of the solvent: lipid bicelles are often used as alignment medium in the measurements of residual dipolar couplings (RDCs); because the ordered liquid crystalline bicellar structure is pressure and temperature dependent,[4,21] it could be destroyed by a rapid pressure change.

The incorporation of a pressure change into the NMR pulse sequence in the PPSCS experiment allows the correlation of structure-dependent NMR parameters at different pressures. A problem here is that the time needed for a pressure step or pulse is significantly larger than the typical transverse relaxation time T_2 of a few milliseconds found in proteins (for very small molecules this is different). Therefore, after the pressure jump the coherence of the system is completely lost. However, the longitudinal relaxation time T_1 of proteins in solution is of the order of seconds, giving the opportunity to store the transverse magnetization for some time as longitudinal magnetization and recreating it after the pressure step. A practical implementation is the addition of a pair of $\pi/2$-pulses with opposite phases

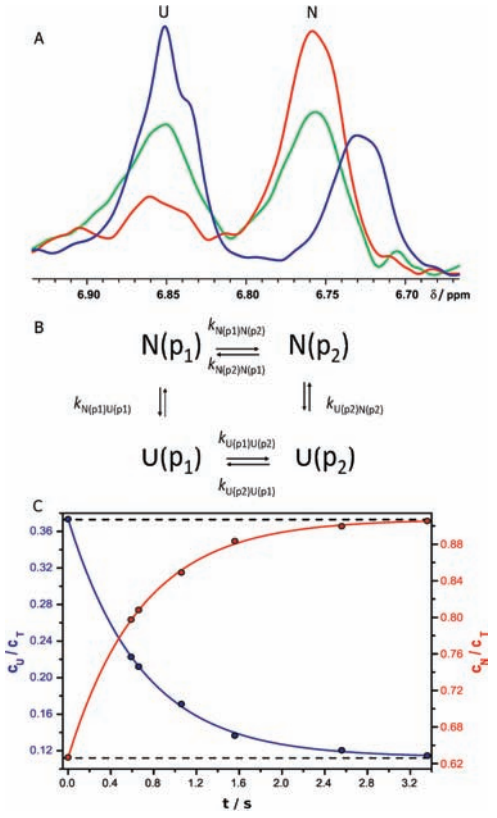

Figure 3. Time dependence of the spectral changes after a pressure perturbation. The sample contained approximately 1.5 mM HPr(I14A) from *S. carnosus* in 10 mM Tris-d_{11}, 0.5 mM EDTA-d_6, 0.5 mM NaN_3, pH 7.0, 99.8% D_2O. Data were measured at T = 285 K. (A) Part of a ^1H NMR spectrum measured at 500.1 MHz showing the H^{ε}-resonance line of Tyr64 in the folded state N and the H^{ε} resonances of all three tyrosine residues of HPr in the unfolded state U. (red) Spectrum at 0.1 MPa, (green) transient after a pressure jump from 80 to 0.1 MPa, (blue) spectrum at 80 MPa. (B) 4-state model used for the description of the experiment. (C) The ratio of the relative concentrations c_U/c_T and c_N/c_T as a function of the time t after the pressure perturbation is plotted as a function of t. c_N, c_U, and c_T are the concentrations of the natively folded protein, the unfolded protein, and the total concentration of the protein. The data were fitted as described in the Experimental Section. Broken lines refer to the equilibrium values.

separated by a time $\tau \ll T_1$, during which the pressure step is performed (Figure 2C and E).

Typical applications would be the transfer of spectral assignments performed in one state (e.g., the well-folded ground state of a protein at ambient pressure) to the spectrum obtained from a different pressure-induced state (e.g., the denatured state or an excited conformational state in slow exchange). Under slow exchange conditions, this allows the recognition (assignment) of the resonances of the second state, but in general it is also helpful in crowded protein spectra under fast exchange conditions. Instead of using a pressure step, a pressure pulse (Figure 2E) could allow one to measure NMR parameters of a perturbed state under conditions where the protein is folded, for example, the interatomic distances in the denatured form of a protein by the intensity of the NOESY cross peaks in the ground state.

For demonstrating that both types of experiments work with the system presented here, a typical PPTSS and a typical PPSCS experiment are presented exemplarily in this Article. The time course of the pressure-induced denaturation/refolding of an active center mutant of HPr protein from *S. carnosus*[7] was observed by one-dimensional NMR spectroscopy after increasing the pressure from ambient pressure to 80 MPa and vice versa. The used pulse sequence is given in Figure 2B. Exemplarily, the resonance lines of the H^{ε}-resonance of Tyr64 in the folded state and of the H^{ε}-resonances of all three tyrosine residues of HPr in the unfolded state are shown. Three different spectra are presented in Figure 3A: a spectrum of HPr in its thermodynamic equilibrium at 0.1 MPa, a spectrum at 80 MPa, and a spectrum obtained 100 ms after decreasing the pressure from 80 to 0.1 MPa. The complete spectra are depicted in the Supporting Information (Figure S2). The relative concentrations of HPr in the folded and unfolded states N and U at a time t after stepping the pressure from p_1 to p_2 can be calculated from the integral of the H^{ε}-resonance of Tyr64 divided by the integral of the resonances of the three tyrosine residues of HPr (Tyr6, Tyr37, Tyr64) in the unfolded state.

In the unfolded state, the latter resonances have the same chemical shift, the random-coil chemical shift. When the time step is much faster than the folding/unfolding transition, the reaction can be described by a four-state model (Figure 3B). In the absence of folding intermediates, the transitions $N(p_1) \leftrightarrow N(p_2)$ and $U(p_1) \leftrightarrow U(p_2)$ after the pressure jump should be very fast because they include only local effects such as slight changes of hydrogen-bond lengths. Experimentally, this assumption can be verified directly, because the chemical shifts after the shortest time t measured correspond already to the chemical shift of HPr in states N and U at the final pressure. The rate constants can be calculated by a fit of the data as (1.29 ± 0.03) and (0.165 ± 0.006) s^{-1} for k_{UN} and k_{NU} at 0.1 MPa (Figure 3C).

Instead of performing a pressure jump from 80 to 0.1 MPa, one can also perform a pressure jump from 0.1 to 80 MPa. From these data, k_{UN} and k_{NU} at 80 MPa can be derived as (0.49 ± 0.05) and (0.20 ± 0.02) s^{-1}, respectively. Pressure influences folding and unfolding kinetics simultaneously, but mainly folding is slowed by pressure. As long as the time required for the pulse sequence itself is shorter than the time scale of the structural rearrangement, more sophisticated 2D-pulse sequences can be used in a PPTSS experiment. For example, the 1D pulse sequence (Figure 2B) can be substituted by any two-dimensional experiment (Figure 2D) such as two-dimensional SOFAST ^1H,^{15}N-HMQC experiments[22] where all amide groups of the protein can be detected separately. This would more or less correspond to the experiments performed manually by the Akasaka group for slow aggregation processes.[3] However, the automation also allows one to perform these experiments in a different way that would still grant a time resolution in the millisecond range (acquisition time for a single low resolution FID; in fact, when only integrals are concerned, the time resolution is even better because the first point of an FID determines the integral): the necessary signal-to-noise ratio can be obtained by repeating the experiment at a given t_1-value N-times and adding the FIDs. A problem could be differences caused by evolution during t_1, an effect that can be avoided by using constant time experiments.[23] Concerning chemical shifts, the time resolution can be further increased by segmental linear prediction of the FIDs.[24]

Rapid pressure changes inside the pulse sequence can be used to correlate spin states at different pressures. An example for such an PPSCS experiment is the application of a pressure jump in a

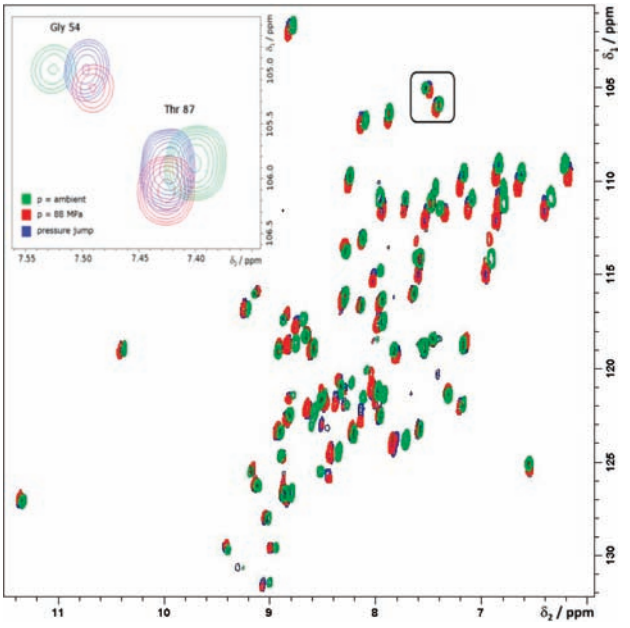

Figure 4. Pressure perturbation state correlation spectroscopy (PPSCS). The sample contained 3 mM of uniformly ^{15}N labeled HPr from *S. aureus* in 90% H_2O/10% D_2O with 0.1 mM DSS as internal standard. The pH was adjusted to 7.0. Small part of the fingerprint region of the PPSCS-^{1}H, ^{15}N HSQC spectrum. (green) Cross peaks at 0.1 MPa, (red) cross peaks at 88 MPa, (blue) correlation peaks with the ^{1}H chemical shifts corresponding to 88 MPa and the ^{15}N chemical shifts corresponding to 0.1 MPa.

^{1}H,^{15}N HSQC at the interface between t_1 and t_2 time evolution (Figure 2D). It allows the correlation of chemical shifts of all protein amide groups at one pressure with the corresponding chemical shifts at another pressure. As an example for such correlation peaks, a small part of such a spectrum is shown in Figure 4 with the correlation peaks (blue) that connect the resonances of Gly54 and Thr87 of the HPr protein from *S. aureus*[25] at low (green) and high pressures (red). Note that the actual pressure used for recording the correlation spectrum was slightly lower than 88 MPa used in the static experiments leading to somewhat smaller ^{1}H chemical shifts changes. Note also the absence of virtually any t_1-noise that would occur when the pressure pulse synchronization with the pulse program and the reproducibility of the pressure slope would not be perfect enough. In addition, the pulse sequences designed here are rather robust against small synchronization errors because the pressure change occurs in a window (typically 100 ms) that is larger than required for the 30 ms pulse step where only *z*-magnetization is relevant. The example shown here is the result observed when fast exchange conditions prevail and assignment of resonances is rather straightforward. Of course, the experiment should also work under slow exchange conditions where assignment is often complicated, for example, when the amide cross peaks of denatured protein have to be assigned to the native state or when the natively folded protein exists in two pressure-sensitive conformational states.

This experiment has similarities to the SCOTCH experiment used by Rubenstenn et al.[26] for the correlation of -amide resonances of photo intermediates of the yellow protein PYP with its ground state. By replacing the laser irradiation by a pressure step, this elegant experiment could give the same information as the experiment described in Figure 4, illustrating also that pressure perturbations can be introduced in many different ways in nD pulse sequences. It should be noted that conceptually the same fundamental classes of experiments were discussed for light-induced transitions[23] that are introduced here for pressure effects.

Rapid temperature changes represent another possibility to increase the dimensionality of the NMR experiments[27] and to perturb the thermodynamic equilibrium. Microwave-induced heating of the sample[28] was used to perform state correlation spectroscopy on liquid crystals as well as on proteins. However, whereas heating by 30 K can be performed in the same millisecond time scale as the pressure changes of 0.08 GPa presented here, cooling of the sample is slow and implies that experiments can be repeated only every 15 min, thus being almost prohibitive for protein work. In addition, repeated heat denaturation usually leads to irreversible aggregation of denatured proteins. In contrast, pressure application can be usually performed many times, because pressure usually enforces dissociation of protein complexes. A complementary method to pressure perturbation is the identification of exchange processes in thermodynamic ensembles by Carr−Purcell like relaxation measurements.[29,30] If measured as a function of the magnetic field, the exchange rates can be fitted with a two-state model: the population of the two states, the exchange correlation times, and the absolute value of the chemical shift difference can be obtained. However, the time scale of the observable dynamics is limited by the transverse relaxation times to values lower than 10 ms, and more complex data including direct 3D structural information cannot be obtained.

In conclusion, we have shown that PPTSS as well as PPSCS can be performed at conditions relevant in protein science. This opens the possibility to perform a wealth of new nD-NMR experiments that provide detailed dynamic and structural information on proteins that is difficult or impossible to obtain with other methods.

■ ASSOCIATED CONTENT

Supporting Information. Details of the high pressure unit and additional spectra. This material is available free of charge via the Internet at http://pubs.acs.org.

■ AUTHOR INFORMATION

Corresponding Author
hans-robert.kalbitzer@biologie.uni-regensburg.de

Present Addresses
[‡]Lipofit Analytic GmbH, Josef-Engert-Strasse 9, 93053 Regensburg, Germany.
[§]Physics Institute of São Carlos, University of São Paulo, Av. Trabalhador Sãocarlense 400, 13566-590 São Carlos, SP, Brazil.

Author Contributions
[†]These authors contributed equally.

■ ACKNOWLEDGMENT

We want to acknowledge financial support from the Deutsche Forschungsgemeinschaft (DFG), the Bayerische Forschungsstiftung, and the Fonds der Chemischen Industrie (FCI).

REFERENCES

(1) Akasaka, K. *Chem. Rev.* **2006**, *106*, 1814–1835.
(2) Kachel, N.; Kremer, W.; Zahn, R.; Kalbitzer, H. R. *BMC Struct. Biol.* **2006**, *6*, doi:10.1186/1472-6807-6-16.
(3) Kitahara, R.; Royer, C.; Yamada, H.; Boyer, M.; Saldana, J.-L.; Akasaka, K.; Roumestand, C. *J. Mol. Biol.* **2002**, *320*, 609–628.
(4) Heuert, U.; Krumova, M.; Hempel, G.; Schiewek, M.; Blume, A. *Rev. Sci. Instrum.* **2010**, *81*, 105102-1–105102-8.
(5) Kalbitzer, H. R.; Kremer, W.; Kachel, N.; Hartl, R.; Ernst, T. *Proc. 47th ENC, Asilomar* **2006**, 17-17.
(6) Maurer, T.; Meier, S.; Kachel, K.; Munte, C. E.; Hasenbein, S.; Koch, B.; Hengstenberg, W.; Kalbitzer, H. R. *J. Bacteriol.* **2004**, *186*, 5906–5918.
(7) Möglich, A.; Koch, B.; Gronwald, W.; Hengstenberg, W.; Brunner, E.; Kalbitzer, H. R. *Eur. J. Biochem.* **2004**, *271*, 4815–4824.
(8) Arnold, M. R.; Kremer, W.; Luedemann, H.-D.; Kalbitzer, H. R. *Biophys. Chem.* **2002**, *96*, 129–140.
(9) Hartl, R. Ph.D. Thesis, University of Regensburg, 2008.
(10) Wishart, D. S.; Bigam, C. G.; Holm, A.; Hodges, R. S.; Sykes, B. D. *J. Biomol. NMR* **1995**, *6*, 135–140.
(11) Sklenar, V.; Piotto, M.; Leppik, R.; Saudek, V. *J. Magn. Reson., Ser. A* **1993**, *102*, 241–245.
(12) Liu, M.; Mao, X.; Ye, C.; Huang, H.; Nicholson, J. K.; Lindon, J. C. *J. Magn. Reson.* **1998**, *132*, 125–128.
(13) Bax, A.; Ikura, M.; Kay, L. E.; Torchia, D. A.; Tschudin, R. *J. Magn. Reson.* **1990**, *86*, 304–318.
(14) Shaka, A. J.; Barker, P. B.; Freeman, R. *J. Magn. Reson.* **1985**, *64*, 547–552.
(15) Woenckhaus, J.; Köhling, R.; Winter, R.; Thiyagarajan, P.; Finet, S. *Rev. Sci. Instrum.* **2000**, *71*, 3895–99.
(16) Yamada, H. *Rev. Sci. Instrum.* **1974**, *45*, 640–642.
(17) Urbauer, J. L.; Ehrhardt, M. R.; Bieber, R. J.; Flynn, P. F.; Wand, A. J. *J. Am. Chem. Soc.* **1996**, *118*, 11329–11330.
(18) Arnold, M. R.; Kalbitzer, H. R.; Kremer, W. *J. Magn. Reson.* **2003**, *61*, 127–131.
(19) Peterson, R. W.; Wand, A. J. *Rev. Sci. Instrum.* **2005**, *76*, 094101-1–094101-7.
(20) Beck Erlach, M.; Munte, C. E.; Kremer, W.; Hartl, R.; Rochelt, D.; Niesner, D.; Kalbitzer, H. R. *J. Magn. Reson.* **2010**, *204*, 196–199.
(21) Brunner, E.; Arnold, M. R.; Kremer, W.; Kalbitzer, H. R. *J. Biomol. NMR* **2001**, *21*, 173–176.
(22) Schanda, P.; Kupce, E.; Brutscher, B. *J. Biomol. NMR* **2005**, *33*, 199–211.
(23) Vuister, G.; Bax, A. *J. Magn. Reson.* **1992**, *98*, 428–435.
(24) Moss, R.; Gesmar, H.; Led, J. J. *J. Am. Chem. Soc.* **1994**, *116*, 747–749.
(25) Maurer, T.; Döker, R.; Görler, A.; Hengstenberg, W.; Kalbitzer, H. R. *J. Bacteriol.* **2004**, *186*, 5906–5918.
(26) Rubinstenn, G.; Vuister, G. W.; Zwanenburg, N.; Hellingwerf, K. J.; Boelens, R.; Kaptein, R. *J. Magn. Reson.* **1999**, *137*, 443–447.
(27) Naito, A.; Nakatani, H.; Imanari, M.; Akasaka, K. *J. Magn. Reson.* **1990**, *87*, 429–432.
(28) Kawakami, M.; Akasaka, K. *Rev. Sci. Instrum.* **1998**, *69*, 3365–3369.
(29) Loria, J. P.; Rance, M.; Palmer, A. G., III. *J. Am. Chem. Soc.* **1999**, *121*, 2331–2332.
(30) Baldwin, A. J.; Kay, L. E. *Nat. Med. Chem.* **2009**, *5*, 808–814.